

# CrystEngComm

Accepted Manuscript



This is an *Accepted Manuscript*, which has been through the Royal Society of Chemistry peer review process and has been accepted for publication.

*Accepted Manuscripts* are published online shortly after acceptance, before technical editing, formatting and proof reading. Using this free service, authors can make their results available to the community, in citable form, before we publish the edited article. We will replace this *Accepted Manuscript* with the edited and formatted *Advance Article* as soon as it is available.

You can find more information about *Accepted Manuscripts* in the [Information for Authors](#).

Please note that technical editing may introduce minor changes to the text and/or graphics, which may alter content. The journal's standard [Terms & Conditions](#) and the [Ethical guidelines](#) still apply. In no event shall the Royal Society of Chemistry be held responsible for any errors or omissions in this *Accepted Manuscript* or any consequences arising from the use of any information it contains.

Cite this: DOI: 10.1039/c0xx00000x

www.rsc.org/crystengcomm

ARTICLE TYPE

# Unique topological motifs in two Cd (II)-coordination polymers: mutual-embedded 2D bilayers, 3D polythreaded structures, self-penetrated network and 2D→2D interpenetrated homochiral bilayers

Guo-Wang Xu<sup>a,b</sup>, Ya-Pan Wu<sup>a</sup>, Hai-Bin Wang<sup>a</sup>, Ye-Nan Wang<sup>a</sup>, Dong-Sheng Li<sup>\*a</sup>, Yun-Ling Liu<sup>\*c</sup>

Received (in XXX, XXX) Xth XXXXXXXXX 20XX, Accepted Xth XXXXXXXXX 20XX

DOI: 10.1039/c0xx00000x

Two unique entangling Cd(II) coordination polymers,  $\{[\text{Cd}_2(m\text{-pdoa})_2(\text{dpa})_3(\text{H}_2\text{O})]\}_n$  (**1**) and  $\{[\text{Cd}(m\text{-pdoa})(\text{bpp})(\text{H}_2\text{O})]\cdot 2\text{H}_2\text{O}\}_n$  (**2**) ( $m\text{-H}_2\text{pdoa}$  = 1,3-phenylenedioxy diacetic acid,  $\text{dpa}$  = 4,4'-dipyridylamine;  $\text{bpp}$  = 1,3-di(4-pyridyl)propane) have been modulated by flexible/semi-rigid mixed aromatic carboxylate and pyridine derivative ligands and characterized by elemental analysis, infrared spectrum (IR), powder X-ray diffraction (PXRD) and single-crystal X-ray diffraction. **1** shows the first topological motifs of mutual-embedded bilayers originating from two reverse 2D  $4^4\text{-sql}$  layers with 1D single side arms in the alternate fashion, and thus affording a 3D polythreaded structure featuring poly-pseudo-rotaxane that exhibits a new 3D (3,3,3,3,3,5,5,5)-connected self-penetrated H-bonding net. Whereas **2** displays a rare 2D→2D homochiral interpenetrated layers propagating from  $4^4\text{-sql}$  chiral layer. Additionally, thermal stabilities and luminescent properties of **1** and **2** were also discussed.

## Introduction

Entangled coordination polymers (CPs) continue to attract remarkable attention in academia and industry due to the endless possibilities and inexhaustible synthesis options for tailoring their structures and properties aimed in various key applications among clean energy, catalysis, sensing, etc.<sup>1</sup> As is well known, entanglements phenomena are common in nature, as seen in catenanes, rotaxanes and molecular knots, and inspired by such fantastic topologies, deversified entangled motifs have been extensively designed and investigated by many CPs's researchers in crystal engineering, however, there still exist many problems need to be solved, such as efficient strategies of synthesis entangled coordination polymers has not been determined, directly relationships between entanglement motifs and properties do not clear enough and so on.<sup>2</sup>

More recently, polythreaded coordination nets, subclass of interpenetrating nets, which can be considered as periodic analogues of the molecular rotaxanes or pseudorotaxanes have drew people's interests for its charming motif and potential applications.<sup>3</sup> In general, the known polythreaded systems can be distinguished into two classes: in the first system, the so-called "polyrotaxane", the different motifs cannot be disentangled without breaking links, and another system contains "separable" motifs.<sup>2a,2d,4,5</sup> The commonly synthesis strategy of polythreading is use flexible carboxylic acid ligands or N-donor molecules to connect the metal ions. In recent years, the employment of mixed ligands during the self-assembly process has gradually become an effective approach, which is expected to obtain many different networks with more diverse structural motifs and desired

properties compared to using only one type of ligands.<sup>6</sup> As a result,

much efforts have been devoted into this hot research field with mixed ligands strategy for the formation of new entangled coordination polymers (CPs).<sup>5,6</sup> Undoubtedly, these meaningful exploitation can significantly enrich our knowledge of assembly processes of these supramolecular architectures and understand subsequent structure-property relationship.

With this background information, we have focused our attention on utilizing aromatic polycarboxylate ligands and N, N'-donor ancillary ligands and different metal ions to generate series of novel coordination polymers with intriguing topological net and interesting properties.<sup>7</sup> Herein, two unique entangling Cd(II) coordination polymers,  $\{[\text{Cd}_2(m\text{-pdoa})_2(\text{dpa})_3(\text{H}_2\text{O})]\}_n$  (**1**),  $\{[\text{Cd}(m\text{-pdoa})(\text{bpp})(\text{H}_2\text{O})]\cdot 2\text{H}_2\text{O}\}_n$  (**2**) ( $m\text{-H}_2\text{pdoa}$  = 1,3-phenylenedioxydiacetic acid,  $\text{dpa}$  = 4,4'-dipyridylamine;  $\text{bpp}$  = 1,3-di(4-pyridyl)propane, Scheme S1) have been synthesized and characterized. Remarkably, **1** contains several unusual characteristics: (i) it represents the first example of mutual-embedded bilayers motif from two reverse  $4^4\text{-sql}$  layer decorated with 1D single side arms in the alternate fashion, (ii) adjacent mutual-embedded 2D layers propagate a 3D polythreaded motifs with the characteristic of poly-pseudo-rotaxane, (iii) considering the strong hydrogen bonds between layers, the resulted network exhibits a 3D (3, 5)-connected self-penetrated net. Compound **2** feature a rare 2D→2D interpenetrated homochiral bilayers consisted of  $4^4\text{-sql}$  chiral layer.

## Experimental Section

### Materials and Physical Measurements

All reagents were commercially available and used without further purification. Elemental analyses for C, H and N were performed on a Flash 2000 organic elemental analyzer. Infrared spectra on KBr pellets were recorded on a Bruker Equinox-55 spectrophotometer in the range 4000–400 cm<sup>-1</sup>. Thermogravimetric analysis was performed on a NETZSCH STA 449C microanalyzer heated from 30 to 750 °C in air atmosphere. Powder X-ray diffraction (PXRD) patterns were taken on a Rigaku Ultima IV diffractometer (Cu K $\alpha$  radiation  $\lambda$  = 1.5406 Å), with a scan speed of 5°/min and a step size of 0.02° in 2 $\theta$ . Fluorescence spectra were recorded on a Hitachi F-4500 fluorescence spectrophotometer at room temperature.

### Preparation of Compound 1 and 2

**{[Cd<sub>2</sub>(m-pdoa)<sub>2</sub>(dpa)<sub>3</sub>(H<sub>2</sub>O)]<sub>n</sub> (1)}** A mixture of dpa (25.7 mg, 0.15 mmol), m-pdoa (22.6 mg, 0.10 mmol), Cd(OAc)<sub>2</sub>·2H<sub>2</sub>O (26.7 mg, 0.10 mmol), NaOH (8.0 mg, 0.20 mmol), and 6 mL deionized water was placed in a Teflon-lined stainless vessel (18 mL). Then the vessel was sealed and heated at 140 °C for 120 h autogenous pressure. After being cooled to room temperature, pale yellow block crystals of **1** were obtained with a yield of 52% based on Cd (II). Anal. Calcd for C<sub>50</sub>H<sub>45</sub>N<sub>9</sub>O<sub>13</sub>Cd<sub>2</sub>: C, 49.97; H, 3.52; N, 10.49%; Found: C, 49.35; H, 3.83; N, 10.57%. IR (KBr pellet, cm<sup>-1</sup>): 3518 (s), 3083 (s), 2910 (s), 2352 (w), 1745 (w), 1582 (m), 1499 (m), 1373 (m), 1339 (s), 1133 (s), 1040 (m), 924 (m), 891 (m), 815 (s), 745 (m), 685 (w).

**{[Cd(m-pdoa)(bpp)(H<sub>2</sub>O)]·2H<sub>2</sub>O} (2)}** **2** was prepared by the similar method as that described for **1**, except that dpa was replaced by bpp (19.8 mg, 0.10 mmol). Pale yellow block crystals were obtained with a yield of 41 % based on Cd(II). Anal. Calcd for C<sub>23</sub>H<sub>28</sub>N<sub>2</sub>O<sub>9</sub>Cd: C, 46.91; H, 4.79; N, 4.76%; Found: C, 46.85; H, 4.83; N, 4.78%. IR (KBr pellet, cm<sup>-1</sup>): 3445 (s), 2920 (s), 2847 (s), 2359 (w), 1582 (s), 1502 (m), 1429 (m), 1349 (m), 1333 (s), 1223 (m), 1180 (s), 1163 (m), 1094 (m), 821 (s), 732 (s), 678 (s).

### X-Ray Crystallography

Single crystal X-ray diffraction data for compound **1** and **2** were collected on a Bruker SMART APEX II CCD diffractometer with graphite-monochromated MoK $\alpha$  radiation ( $\lambda$  = 0.71073 Å) at room temperature. The structures were solved using direct methods and successive Fourier difference synthesis (SHELXL-2014/7), and refined using the full-matrix least-squares method on  $F^2$  with anisotropic thermal parameters for all non-H atoms (SHELXL-2014/7). The hydrogen atoms were assigned with common isotropic displacement factors and included in the final refinement by use of geometrical restraints. The H atoms of coordinated water molecules were located using the difference Fourier method and refined freely. Details of the crystal parameters, data collection, and refinements for **1–2** are listed in Table 1 and Table S1. CCDC Nos: 1059146 for **1**, 1059147 for **2**.

## Results and Discussion

### Synthetic Chemistry

Aiming to explore different kind of N-donor bridging ligands mediation on assembly and structural variability of the entangled coordination polymers, a series of hydrothermal strategies were

attempted to disclose the crucial factor. In the similar hydrothermal reaction system, dpa, bpp, imidazole (im), 1,5-bis(imidazol)pentane (bip), 1,2-bis(imidazol)ethane (bie), 1,6-bis(imidazol)hexane (bih), pyridine (py), 1,4-bis(imidazol)butane (bib), 1,4-bis(imidazolyl-1-methyl)-benzene (bix), as N-donor bridging ligands were selected, respectively. The results show that only when dpa, bpp, im, py, bib, and bix were used as N-donor ligands, correspondingly crystalline products **1**, **2**, [Cd(m-pdoa)(im)<sub>2</sub>]<sub>n</sub> (IUCr: HB6123), (**3**); [Cd(m-pdoa)(py)(H<sub>2</sub>O)]<sub>n</sub> (CCDC: 235936), (**4**); {[Cd(m-pdoa)(bix)]·3H<sub>2</sub>O}<sub>n</sub> (CCDC: 932841) (**5**) and [Cd(m-pdoa)(bix)]<sub>n</sub> (CCDC: 932840) (**6**) were obtained.<sup>8</sup> Inversely, other three auxiliary ligands (bip, bie and bih) could not get crystal in the similar conditions.

**Table 1** Crystal data and structure refinements for **1** and **2**

| Compound   | <b>1</b>   | <b>2</b>   |
|--|--|--|
| empirical formula  | C <sub>50</sub> H <sub>45</sub> N <sub>9</sub> O <sub>13</sub> Cd <sub>2</sub> | C <sub>23</sub> H <sub>28</sub> N <sub>2</sub> O <sub>9</sub> Cd |
| formula weight   | 1204.75  | 588.87   |
| crystal system   | Monoclinic   | Monoclinic   |
| space group  | <i>P</i> 2 <sub>1</sub> / <i>c</i>   | <i>C</i> 2/ <i>c</i>   |
| <i>a</i> (Å)   | 17.6240(11)  | 21.234(9)  |
| <i>b</i> (Å)   | 11.8156(7)   | 15.744(6)  |
| <i>c</i> (Å)   | 26.1460(13)  | 16.213(7)  |
| $\beta$ (°)  | 116.317(3)   | 113.443(4)   |
| Volume (Å <sup>3</sup> )   | 4880.3(5)  | 4973(3)  |
| <i>Z</i>   | 4  | 8  |
| <i>T</i> (K)   | 296(2)   | 296(2)   |
| <i>D</i> <sub>c</sub> (g·cm <sup>-3</sup> )  | 1.640  | 1.573  |
| $\mu$ (mm <sup>-1</sup> )  | 0.948  | 0.932  |
| <i>F</i> (000)   | 2432   | 2400   |
| data collected   | 11760  | 4168   |
| independent data   | 9937   | 2401   |
| <i>R</i> <sub>int</sub>  | 0.0237   | 0.0619   |
| goodness-of-fit  | 1.020  | 1.065  |
| <i>R</i> <sub>1</sub> <sup>a</sup> , <i>wR</i> <sub>2</sub> <sup>b</sup> [ <i>I</i> > 2 $\sigma$ ( <i>I</i> )] | 0.0345, 0.0872   | 0.0867, 0.2204   |
| <i>R</i> <sub>1</sub> , <i>wR</i> <sub>2</sub> (all data)  | 0.0423, 0.0919   | 0.1457, 0.2975   |

$$^a R = \sum ||F_o| - |F_c|| / \sum |F_o|; ^b wR_2 = [\sum [w(F_o^2 - F_c^2)^2] / \sum (F_o^2)]^{1/2}$$

Previous studies have shown that the formation of entangled coordination polymers relies on subtle changes in various hydrothermal parameters especially N-donor ligands.<sup>9</sup> In this work, when the reaction system was determined, compared with other six kinds of N-donor ligands above-mentioned, dpa/bpp ligands play key roles in governing the final structures. So it can be speculated that the long flexible N-donor ligand might act as auxiliary to facilitate the formation of interpenetrated networks and influence the structures of the crystal.

Compounds **1** and **2** are stable in common organic solvents and can retain their crystalline integrity at air ambient condition for a long time. The IR spectra of **1** and **2** shows strong absorption bands between 1619 and 1356 cm<sup>-1</sup>, and no characteristic absorption band of COOH in the range of 1705–1725 cm<sup>-1</sup> is observed, indicating a complete deprotonation of the m-pdoa ligand. The broad bands at region of 3300–3600 cm<sup>-1</sup> associated with the O–H stretching vibrations of water molecules

and/or noncoordinated water, which it is also confirmed by the X-ray crystal structure.

### Description of Crystal Structures

$\{[\text{Cd}_2(\text{m-pdoa})_2(\text{dpa})_3(\text{H}_2\text{O})]\}_n$  (**1**). X-ray structural analysis reveals that **1** crystallizes in monoclinic space group  $P2_1/n$ , and the asymmetric unit consists of two Cd (II) ions with different coordination geometries, two *m-pdoa*<sup>2-</sup> anions, three dpa ligands, and one coordinated water. As shown in Fig. 1, the Cd1 center displays a distorted octahedral sphere surrounded by three carboxylate-O (O2, O3, O4) from different *m-pdoa*<sup>2-</sup>, two nitrogen atoms (N7 and N9#4, symmetry code: #4:  $x+3/2, -y+3/2, z+1/2$ ) from two dpa and one coordinated water (O1). Analogously, the Cd2 center connects six atoms that are three carboxylate-O (O8, O10, O11) from different *m-pdoa*<sup>2-</sup> and three nitrogen atoms (N3, N4 and N6#2 symmetry codes: #2:  $x, y-1, z$ ) from three dpa molecules. All Cd–O bond lengths are comparable to those reported in the literature, although the length of Cd1–O2 bond (2.528 Å) is slightly longer than that of other Cd–O bonds (2.242–2.421 Å).<sup>10</sup>

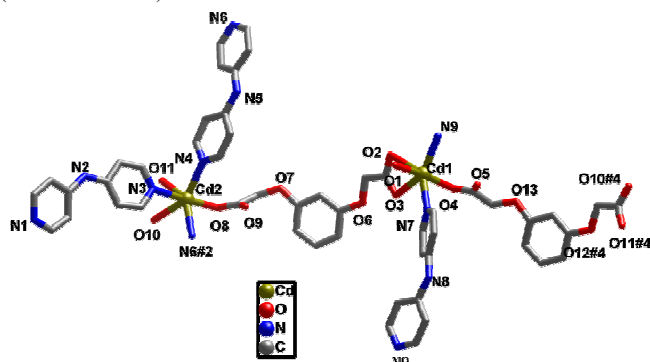


**Fig. 1** Coordination environment of Cd (II) atoms in **1**; hydrogen atoms are omitted for clarity. Symmetry codes: #2:  $x, y-1, z$ ; #4:  $x+3/2, -y+3/2, z+1/2$ .

In **1**, the adjacent Cd (II) ions are bridged by *m-pdoa*<sup>2-</sup> ions to form a 1D chain, and then the chains are further linked by dpa molecules to form an infinite 2D undulate 4<sup>4</sup>-*sql* layer. Obviously, there exist two kinds of large windows named  $W_1$  and  $W_2$ , which built up by four Cd(II) ions, two *m-pdoa* ligands and dpa molecules with dimensions of 17.833×17.631 Å and 19.654×15.554Å (Fig. S1), respectively. Interestingly, at the middle of the rhombic edge, dangling dpa ligands are coordinated to the sole Cd2, lying in an axial orientation, generating the first example of 2D layer with 1D single side arms in the alternate fashion (Fig. 2a and 2b). More interestingly, two reverse adjacent layers are mutual-embedded and resulting in the 2D embraced bilayers with the alternatively lateral arms hanging on both sides of the layers (Fig. 2c). Additionally, the adjacent layers take a parallel stacking and arrange in an offset fashion seen in a view along the [101] direction with a near repeat sequence of ABAB. And the distance between the adjacent layers is about 4.580Å (from Cd (II) center to the center of benzene ring among the adjacent layer), and the length of lateral arm is about 9.972Å (from one Cd (II) ions to the uncoordinated terminal nitrogen of dpa, as shown in Fig. 2c and Fig. 2e). The most fascinating structural feature of **1** is that the dangling dpa groups are just like open arms protruding from single side of the sheets, and all the bilayers are stacked parallel

and arranged in a staggered fashion, which forms a 3D polythreaded topological motifs (Fig. 2f).

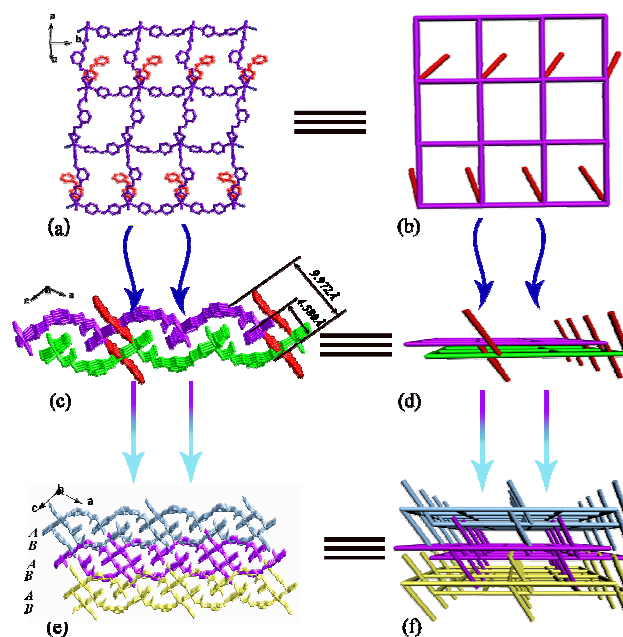


**Fig. 2** Structure of **1**: (a) 2D undulate 4<sup>4</sup>-*sql* layer with side arms; (b) model of single layer with side arms in the alternate fashion; (c) mutual-embedded 2D bilayers; (d) schematic diagram 2D bilayers; (e) 3D polythreaded topological motifs with a near repeat sequence of ABAB; (f) schematic representation of 3D polythreaded motifs.

Additionally, the threading layers are reinforced by strong hydrogen bonding interactions between the nitrogen atoms of dpa from one lateral arm, carboxyl oxygen atoms from the other layer and coordinated water molecules ( $\text{O}\cdots\text{O}$ , 2.825 Å,  $\text{O}\cdots\text{N}$ , 2.722Å). There exist N5–H5A $\cdots$ O9, N2–H2A $\cdots$ O5, and O7–H7A $\cdots$ O1 bonds between such two 2D layers. Topologically, when these hydrogen bonds are taken into account, the two Cd(II) centers and one  $L_A$  ligand (involving C4 atom) can be regarded as the five-connected nodes and all other organic ligands as the three-connected nodes, respectively ( $L_A$  = dicarboxyl). As a result, a 8-nodal (3,3,3,3,3,5,5,5)-connected hydrogen bonded topological nets with the point symbol of (4.5.6<sup>4</sup>.7<sup>3</sup>.8)(4.5.6<sup>6</sup>.7.8)(4.5.7)<sub>2</sub>(5.7<sup>2</sup>)(6<sup>2</sup>.7)(6<sup>2</sup>.8)(6<sup>4</sup>.7<sup>2</sup>.8<sup>2</sup>.10.11) is formed (Fig. 3(a)), this is a new topological networks via searching in the latest TTO database according to the TOPOS program<sup>11</sup>. Notably, this structure represents a self-penetrating network prototype, in which the eight-membered circuit consisting of two Cd1, two Cd2, two  $L_A$ , and two  $L_N$  nodes are penetrated by the  $L_A$ – $L_N$  rod and ( $L_N$  = pyridyl amine), as shown in Fig. 3b, the nature of the entanglement in **1** can be attributed to poly-pseudo-rotaxane.

So far, only six 2D→3D polythreaded with side arms frameworks have been reported:  $[\text{Zn}(\text{HBTC})(4,4'\text{-bipy})]_n$  (CCDC:233352) (**3**),  $[(\text{Ni}_3(\text{oba})_2(4,4'\text{-bipy})_2(\text{Hoba})_2(\text{H}_2\text{O})_2)\text{bpy}\cdot 2\text{H}_2\text{O}]$  (CCDC:266681) (**4**),  $[\text{Cd}(\mu\text{-tp})(\mu\text{-bpp})_2(\text{bpp})_2\text{Br}_2]_n$  (CCDC:669360) (**5**),  $[\text{Cu}_4(\text{bpt})_4(\text{oba})_4(\text{H}_2\text{O})_2]_n\cdot 7\text{H}_2\text{O}$  (CCDC: 716778) (**6**) and  $[\text{Ni}_2(\text{Tipa})_2(\text{L}_1)_2(\text{H}_2\text{O})_2]\cdot 3.25\text{H}_2\text{O}$  (CCDC:14008) (**7**)<sup>2c, 12</sup>. In the reported compounds of **3**–**7**, the 3D polythreaded topological motifs are all constructed from single 2D layers with



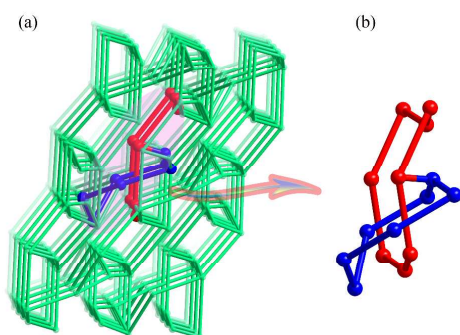


**Fig. 3** View of the topology net of **1**: (a) 8-nodal (3,3,3,3,3,5,5,5)-connected hydrogen bonded topological net; (b) a view of the lateral arms of one polyrotaxane layer passed into the vacant 8-membered loops of an adjacent polyrotaxane layer.

dangling ligand arms. Generally speaking, there are two distinguishing features in the formation of single 2D layers with side arms. One is the dangling pendants embellishing the same side, the other is the side arms locating in the two sides of 2D layer up and down. Contrastively, **1** possess several unusual features: it is the first time that the 1D single side arms in the alternate fashion have been introduced into 2D undulate  $4^4$ -*sql* layer; additionally, adjacent mutual-embedded 2D layers form embraced bilayers and thus affording a 3D polythreaded topological motifs with the characteristic of poly-pseudo-rotaxane, finally, considering the hydrogen bonding interaction between the embraced bilayers, the resultant structure displays a novel 3D 8-nodal (3,5)-connected self-penetrating networks.

$\{[\text{Cd}(\text{m-pdoa})(\text{bpp})(\text{H}_2\text{O})] \cdot 2\text{H}_2\text{O}\}_n$  (**2**). When dpa was replaced by a longer bpp ligand, an unusual 2D  $\rightarrow$  2D interpenetrated networks could be obtained. The asymmetric unit of **2** contains one independent Cd(II) ion, one *m*-pdoa anion, one bpp ligand and one water molecule (Fig. 4). The Cd1 center is coordinated by five oxygen atoms from *m*-pdoa anions and coordinated water (O1, O2, O5#2, O6#2, O7#2; symmetry code:  $x-1/2, y+1/2, z$ ) and two N atoms from bpp molecules (N1 and N2#1; symmetry code:  $x-1/2, y-1/2, z$ ), respectively. The Cd–O bond lengths are in a range of 2.297–2.567, which is close to that of compound **1**.

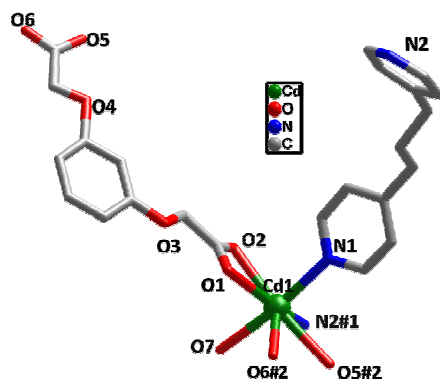


**Fig. 4.** Coordination environment of Cd(II) atoms in **2**; hydrogen atoms are omitted for clarity. Symmetry codes: #1:  $x-1/2, y-1/2, z$ ; #2:  $x-1/2, y+1/2, z$ .

Detailed structural analysis reveals that compound **2** contains a couple of heterochiral bilayers. Due to the bridging style of the *m*-pdoa ligands and bpp molecules, the Cd(II) centers are linked by such spacers to afford a 2D grid-like network with the familiar  $4^4$ -*sql* layer in the *ab* plane (Fig. 5b). Interestingly, the adjacent Cd(II) ions are linked by alternately *m*-pdoa anions and bpp ligands to form a single right-/left-handed helical chain with a helical pitch of 15.745 Å along the *b* axis (Fig. 5a and Fig. 5f). Moreover, the adjacent chains are inter connected by Cd(II) ions to form the infinite homochiral layer (Fig. 5b and Fig. 5g). In the layer, two *m*-pdoa anion, two bpp molecules and four Cd(II) ions form a repeating rhombic grid with a side length of  $13.217 \times 13.217$  Å, a diagonal measurement of  $15.745 \times 21.234$  Å based on the metal–metal distances. Due to the flexibility or length of the *m*-pdoa and bpp ligands, two independent  $4^4$ -*sql* layer are interpenetrating each other in a parallel fashion, generating an infinite 2D double-layer structure with the same handedness (Fig. 5c and 5h). Noteworthy is that the adjacent double-layers exhibit opposite chirality and extend parallel to the *ab* plane, and further are stacking into a 3D achiral structure (Fig. 5e, Fig. S2)

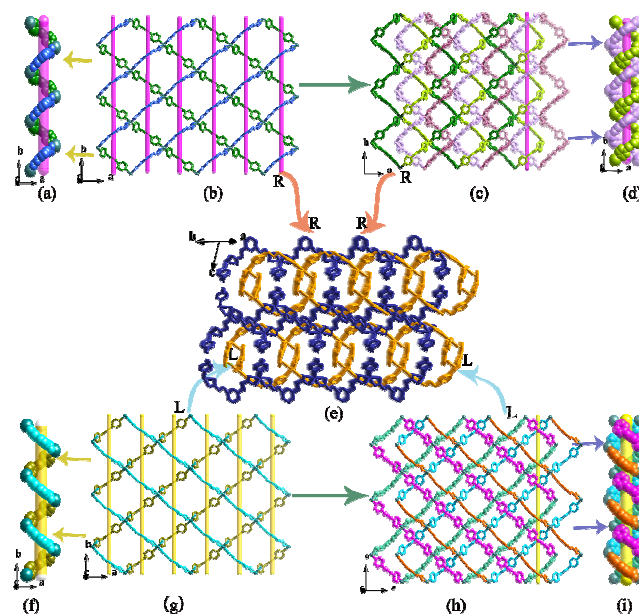


**Fig. 5** View of entangled structure of **2**: (a) right-handed helical chains; (b) single homochiral layer; (c) interpenetrating homochiral double-layers; (d) double-stranded right-handed helical chains; (e) 3D achiral structure; (f) left-handed helical chains; (g) single homochiral layer; (h) interpenetrating homochiral double-layers; (i) double-stranded left-handed helical chains (R represents right-handed with dark blue and L represents left-handed with yellow).

Helices are of intense interest because living organisms utilize them to store and transmit genetic information as protein bundles and DNA and are prevalent in biological systems.<sup>13</sup> More importantly, these helical compounds have many characteristic features and broad applications in the fields of chiral synthesis, optical devices, sensory functions, and so forth.<sup>13a, 14</sup> Recently, some single-, double-, triple-, and higher order helical complex

have been obtained.<sup>14a, 15</sup> However, to the best of our knowledge, few examples in which there are helical chains constructed by mixed ligands and two layers interpenetrated with each other in a parallel fashion, making an infinite 2D double-layer structure with the same handedness, have been reported. A latest Cambridge Structural Database (CSD) search (version 5.33, 2015) revealed that there are only few similar complexes such as:  $[\text{Cd}_2(\text{CH}_3\text{O-ip})_2(1,3\text{-btp})_2(\text{H}_2\text{O})_2]\cdot 7\text{H}_2\text{O}$  (CCDC:850774), (**8**),  $[\text{Cd}(\text{L})(\text{CH}_3\text{OH})(\text{H}_2\text{O})]_n$  (CCDC:869046), (**9**),  $\{[\text{Cd}(\text{cpds})(\text{bpa})_{1.5}]\cdot 3\text{H}_2\text{O}\}_n$  (CCDC:793997), (**10**),  $[\text{Zn}(\text{mpdc})(\text{bpp})]\cdot 2.5\text{H}_2\text{O}$  (CCDC:891545), (**11**),  $[\text{Zn}(\text{abda})(\text{bimh})]_n$  (CCDC:832029), (**12**).<sup>9a, 15</sup> Compounds **8-12** were constructed by a single chiral layer and the near layers show opposite handedness. Compound **2** is another new example of network that contains a homochiral bilayer featuring double helical motifs, and the alternating stacking of oppositely handedness bilayers renders racemic.

### Structural comparison of **1** and **2**

As discussed above, compound **1** and **2** constructed the same carboxylate ligand but with different N-donor ligand and show the different 3D structures. Although the *m*-pdoa<sup>2-</sup> anions take different bridging modes, such as  $\mu_2\text{-}\eta^1\text{:}\eta^1\text{:}\eta^1$  (for **1**),  $\mu_2\text{-}\eta^1\text{:}\eta^1\text{:}\eta^1\text{:}\eta^1$  (for **2**) fashions (Scheme S2), the Cd $\cdots$ Cd distance separated by *m*-pdoa<sup>2-</sup> anions is almost identical (13.236 and 13.224 Å in **1**, 13.217 Å for **2**). In fact, **1** and **2** were prepared under similar hydrothermal conditions, they show different 3D coordination frameworks mainly due to the present of various N-donor ligands. In our previous work, we have reported two kinds of Cd(II) coordination polymers synthesized by *m*-pdoa and different N-donors, the resulting networks show the tremendously different.<sup>8d</sup> In this sense, the different length, flexibility and shape of the two N-donor bridging ligands play important roles in governing the coordination motifs and the final structures.

### PXRD and Thermal Stabilities

In order to check the phase purity of the bulk materials for **1** and **2**, powder X-ray diffraction (PXRD) patterns were recorded at room temperature. As shown in Fig. S3 and Fig. S4, the peak positions of the simulated and experimental PXRD patterns are in agreement with each other, which confirm their phase purity. The difference in intensity of some diffraction peaks may be attributed to the preferred orientation of the crystalline powder samples.

To examine the thermal stability of **1** and **2**, TGA experiments were performed by heating the numerous single crystals in the 30–750°C temperature (Fig. S5). Compound **1** loses one lattice water before 100°C and keeps stable up to 225°C. After about 230°C, the composition of the framework begins to collapse and the final mass remnant of 21.61% at 600 °C represents the deposition of CdO (21.37% calcd). In contrast to **1**, compound **2** loses the lattice and coordinated water molecules at 95–135°C (calc. 9.17% and exp. 9.37%), and the residue remains unchanged until 230°C, the final production is CdO (calc. 21.80% and exp. 23.78%) (Fig. S5).

### Photoluminescence Properties

The photoluminescence spectra of **1** and **2** were examined in the solid state at room temperature. According to the

previous study, it is found that the emission bands for the free *m*-H<sub>2</sub>pdoa ligand and bpp display photoluminescence emission at about 394 nm, 508 nm respectively, no clear luminescence was detected for dpa.<sup>8d, 16b, 17</sup> The emission bands of these free organic ligands can be assigned to the  $\pi^*\rightarrow n$  or  $\pi^*\rightarrow\pi$  transition. The emission spectra show maximum emission peaks at 349 nm ( $\lambda_{\text{ex}}=289$  nm) for **1**, 335 nm ( $\lambda_{\text{ex}}=251$  nm) for **2**, respectively (Fig. S6). They may be assigned to a mixture characteristics of intraligand ( $\pi^*\rightarrow n$  or  $\pi^*\rightarrow\pi$  transition) and ligand-to-ligand charge transition (LLCT), as reported for other Cd(II)-based metal-organic frameworks constructed from mixed N/O-donor ligands. The enhancement of luminescence may be attributed to ligand chelation to the metal center which effectively increases the rigidity of the ligand and reduces the loss of energy by radiationless decay. The difference of the emission behaviors for **1** and **2** probably derive from the differences in the rigidity of solid-state crystal packing.

### Conclusions

In summary, two unique entangling Cd(II) coordination polymers have been prepared by mixed ligands system. **1** represents the first example of mutual-embedded bilayers motif that was self-assembled from two reverse 2D 4<sup>4</sup>-*sql* layer with 1D single side arms in the alternate fashion, further propagating a 3D polythreaded poly-pseudo-rotaxane motifs and a 3D (3, 5)-connected self-penetrated H-bonding net. **2** is a rare 2D→2D homochiral interpenetrated layers consisted of 4<sup>4</sup>-*sql* chiral layer. The two compounds show varied degree photoluminescent emission due to different rigidity of structures. The results will promote us to design new crystalline materials with special topological networks and properties utilizing flexible/semi-rigid mixed aromatic carboxylate and pyridine derivative systems.

### Acknowledgments

This work was financially supported by the NSF of China (Nos. 21201109, 21373122, and 21301106), the Project of Hubei PEO (Nos. Q20131304 and Q20141201), the NSF of Hubei (2014CFB277), the Graduate Student Research Innovation Fund of CTGU (CX2014094) and Training Excellent Master's Thesis Fund of CTGU (Nos. PY2015074).

### Notes and references

- <sup>95</sup> <sup>a</sup>College of Materials and Chemical Engineering, Hubei Provincial Collaborative Innovation Center for New Energy Microgrid, China Three Gorges University, Yichang, 443002, China. Tel./Fax: +86-717-6397506; E-mail address: lidongsheng1@126.com (D.-S. Li).
- <sup>100</sup> <sup>b</sup>College of Science, China Three Gorges University, Yichang, 443002, China
- <sup>105</sup> <sup>c</sup>State Key Laboratory of Inorganic Synthesis and Preparative Chemistry, College of Chemistry, Jilin University, Changchun 130012, P. R. China. E-mail address: yunling@jlu.edu.cn (Y.-L. Liu)
- <sup>110</sup> <sup>†</sup>Electronic Supplementary Information (ESI) available: Crystallographic data in CIF format, selected bond lengths and bond angles, PXRD patterns, TG curves, photoluminescence emission spectra and other supplementary figures for **1** and **2**. These data can be obtained free of charge from The Cambridge Crystallographic Data Centre via [www.ccdc.cam.ac.uk/data\\_request/cif](http://www.ccdc.cam.ac.uk/data_request/cif). See DOI: 10.1039/c0ce000000/

- 1 (a) L. Carlucci, G. Ciani, D. M. Proserpio, T. G. Mitina, V. A. Blatov, *Chem. Rev.* 2014, **114**, 7557; (b) H.-C. Zhou, J. R. Long, O. M. Yaghi, *Chem. Rev.* 2012, **112**, 673; (c) H. Furukawa, K. E. Cordova, M. O'Keeffe, O. M. Yaghi, *Science* 2013, **341**, 1230444; (d) M. Du, C.-P. Li, M. Chen, Z.-W. Ge, X. Wang, L. Wang, C.-S. Liu, *J. Am. Chem. Soc.* 2014, **136**, 10906; (e) X.-Z. Song, S.-Y. Song, S.-N. Zhao, Z.-M. Hao, M. Zhu, X. Meng, L.-L. Wu, H.-J. Zhang, *Adv. Funct. Mater.* 2014, **24**, 4034.
- 2 (a) J. Yang, J.-F. Ma, S. R. Batten, *Chem. Commun.* 2012, **48**, 7899; (b) X.-L. Wang, C. Qin, E.-B. Wang, L. Xu, Z.-M. Su, C.-W. Hu, *Angew. Chem.* 2004, **116**, 5146; (c) X. L. Wang, C. Qin, E. B. Wang, Y. G. Li, Z. M. Su, L. Xu, L. Carlucci, *Angew. Chem. Int. Ed. Engl.* 2005, **44**, 5824; (d) L. Carlucci, G. Ciani, D. M. Proserpio, *Coord. Chem. Rev.* 2003, **246**, 247; (e) H.-B. Zhang, P. Lin, E.-X. Chen, Y.-X. Tan, T. Wen, A. Aldalbahi, Y. Yamauchi, S.-W. Du, J. Zhang, *Chem. Eur. J.* 2015, **21**, 4931; (f) X. Meng, S.-Y. Song, X.-Z. Song, M. Zhu, S.-N. Zhao, L.-L. Wu, H. J. Zhang, *Chem. Commun.* 2015, **51**, 8150-8152.
- 3 (a) T. Cao, Y. Peng, T. Liu, S. Wang, J. Dou, Y. Li, C. Zhou, D. Li, J. Bai, *CrystEngComm* 2014, **16**, 10658; (b) Y.-L. Gai, F.-L. Jiang, L. Chen, Y. Bu, M.-Y. Wu, K. Zhou, J. Pan, M.-C. Hong, *Dalton Trans.* 2013, **42**, 9954; (c) W.-Q. Kan, J. Yang, Y.-Y. Liu, J.-F. Ma, *Inorg. Chem.* 2012, **51**, 11266; (d) X. Zhu, P.-P. Sun, J.-G. Ding, B.-L. Li, H.-Y. Li, *Cryst. Growth Des.* 2012, **12**, 3992; (e) W. Xia, P. Tang, X.-Q. Wu, J. Cui, D.-S. Li, W.-W. Dong, J. Y. Lu, *Inorg. Chem. Commun.* 2015, **51**, 17.
- 4 Q.-X. Yao, Z.-F. Ju, X.-H. Jin, J. Zhang, *Inorg. Chem.* 2009, **48**, 1266.
- 5 (a) X. He, X.-P. Lu, M.-X. Li, R. E. Morris, *Cryst. Growth Des.* 2013, **13**, 1649; (b) X. Wang, H. Hu, A. Tian, H. Lin, J. Li, *Inorg. Chem.* 2010, **49**, 10299; (c) J.-X. Yang, Y.-Y. Qin, J.-K. Cheng, Y.-G. Yao, *Cryst. Growth Des.* 2014, **14**, 1047; (d) J.-J. Shen, M.-X. Li, Z.-X. Wang, C.-Y. Duan, S.-R. Zhu, X. He, *Cryst. Growth Des.* 2014, **14**, 2818.
- 6 (a) J. Gao, M. He, Z. Y. Lee, W. Cao, W. W. Xiong, Y. Li, R. Ganguly, T. Wu, Q. Zhang, *Dalton Trans* 2013, **42**, 11367; (b) M. Chen, E. C. Sañudo, E. Jiménez, S.-M. Fang, C.-S. Liu, M. Du, *Inorg. Chem.* 2014, **53**, 6708; (c) J. Wang, X. Zhu, Y.-F. Cui, B.-L. Li, H.-Y. Li, *CrystEngComm* 2011, **13**, 3342; (d) Y.-Y. Liu, Z.-H. Wang, J. Yang, B. Liu, Y.-Y. Liu, J.-F. Ma, *CrystEngComm* 2011, **13**, 3811; (e) Y.-F. Cui, X. Qian, Q. Chen, B.-L. Li, H.-Y. Li, *CrystEngComm* 2012, **14**, 1201.
- 7 (a) D.-S. Li, Y.-P. Wu, P. Zhang, M. Du, J. Zhao, C.-P. Li, Y.-Y. Wang, *Cryst. Growth Des.* 2010, **10**, 2037; (b) D.-S. Li, J. Zhao, Y.-P. Wu, B. Liu, L. Bai, K. Zou, M. Du, *Inorg. Chem.* 2013, **52**, 8091; (c) D.-S. Li, Y.-P. Wu, J. Zhao, J. Zhang, J. Y. Lu, *Coord. Chem. Rev.* 2014, **261**, 1; (d) J. Zhao, Y. Wang, W. Dong, Y. Wu, D. Li, B. Liu, Q. Zhang, *Chem. Commun.* 2015, **51**, 9479; (e) J. Zhao, W.-W. Dong, Y.-P. Wu, Y.-N. Wang, C. Wang, D.-S. Li, Q.-C. Zhang, *J. Mater. Chem. A*, 2015, **3**, 6962.
- 8 (a) S. Gao, J.-W. Liu, L.-H. Huo, H. Zhao, J.-G. Zhao, *Acta Crystallogr. Sec. E* 2004, **60**, m1878; (b) S. Gao, J.-W. Liu, L.-H. Huo, H. Zhao, J.-G. Zhao, *Acta Crystallogr. Sect. E* 2004, **60**, m1875; (c) S. Gao, J.-W. Liu, S. W. Ng, *Appl. Organomet. Chem.* 2004, **18**, 413; (d) J. Zhao, D. S. Li, Y. P. Wu, W. W. Dong, L. Bai, J. Y. Lu, *Inorg. Chim. Acta* 2014, **413**, 6.
- 9 (a) Y.-F. Hou, Y. Yu, K.-F. Yue, Q. Wei, Y.-L. Liu, C.-S. Zhou, Y.-Y. Wang, *CrystEngComm* 2013, **15**, 7161; (b) H. Wu, X.-L. Lu, C.-L. Yang, C.-X. Dong, M.-S. Wu, *CrystEngComm* 2014, **16**, 992; (c) S. Su, C. Qin, Z. Guo, H. Guo, S. Song, R. Deng, F. Cao, S. Wang, G. Li, H. Zhang, *CrystEngComm* 2011, **13**, 2935; (d) H. Chen, D. Xiao, L. Fan, J. He, S. Yan, G. Zhang, D. Sun, Z. Ye, R. Yuan, E. Wang, *CrystEngComm* 2011, **13**, 7098.
- 10 (a) S.-T. Zheng, T. Wu, F. Zuo, C. Chou, P. Feng, X. Bu, *J. Am. Chem. Soc.* 2012, **134**, 1934; (b) L. Wang, Y.-A. Li, F. Yang, Q.-K. Liu, J.-P. Ma, Y.-B. Dong, *Inorg. Chem.* 2014, **53**, 9087; (c) X. Zhu, N. Wang, X. Xie, R. Hou, D. Zhou, Y. Li, J. Hu, X. Li, H. Liu, W. Nie, *RSC Adv.* 2014, **4**, 15816; (d) L.-L. Liu, C.-X. Yu, Y.-R. Li, J.-J. Han, F.-J. Ma, L.-F. Ma, *CrystEngComm* 2015, **44**, 1636.
- 11 V. A. Blatov, *Struct. Chem.*, 2012, **23**, 955.
- 12 (a) C. Qin, X. Wang, L. Carlucci, M. Tong, E. Wang, C. Hu, L. Xu, *Chem Commun.* 2004, 1876; (b) G.-H. Wang, Z.-G. Li, H.-Q. Jia, N.-H. Hu, J.-W. Xu, *Cryst. Growth Des.* 2008, **8**, 1932; (c) G.-L. Wen, Y.-Y. Wang, Y.-N. Zhang, G.-P. Yang, A.-Y. Fu, Q.-Z. Shi, *CrystEngComm* 2009, **11**, 1519; (d) H. Wu, B. Liu, J. Yang, H.-Y. Liu, J.-F. Ma, *CrystEngComm* 2011, **13**, 3661.
- 13 (a) G.-Y. Wang, C. Song, D.-M. Kong, W.-J. Ruan, Z. Chang, Y. Li, *J. Mater. Chem. A* 2014, **2**, 2213; (b) B. Moulton, M. J. Zaworotko, *Chem. Rev.* 2001, **101**, 1629; (c) C. Schmuck, *Angew. Chem. Int. Ed.* 2003, **42**, 2448.
- 14 (a) H.-T. Zhang, J.-W. Zhang, G. Huang, Z.-Y. Du, H.-L. Jiang, *Chem. Commun.* 2014, **50**, 12069; (b) W. Zhao, L. Chen, H.-M. Li, D.-J. Wang, D.-S. Li, T. Chen, Z.-P. Yuan, Y.-J. Tang, *Biorg. Med. Chem.* 2014, **22**, 2998; (c) B. Zheng, C. Wang, C. Wu, X. Zhou, M. Lin, X. Wu, X. Xin, X. Chen, L. Xu, H. Liu, J. Zheng, J. Zhang, S. Guo, *J. Phys. Chem. C* 2012, **116**, 15839; (d) Y. Takezawa, M. Shionoya, *Acc. Chem. Res.* 2012, **45**, 2066.
- 15 (a) W. Sun, C. Zhang, H. Ma, H. Pang, S. Li, *Dalton Trans.* 2014, **43**, 16322; (b) L. Gomez-Hortiguera, T. Alvaro-Munoz, B. Bernardo-Maestro, J. Perez-Pariente, *Phys. Chem.* 2015, **17**, 348; (c) Z.-H. Zhang, Q.-Q. Zhang, S. Feng, Z.-J. Hu, S.-C. Chen, Q. Chen, M.-Y. He, *Dalton Trans.* 2014, **43**, 646; (d) X. Zhang, L. Fan, W. Zhang, Y. Ding, W. Fan, X. Zhao, *Dalton Trans.* 2013, **42**, 16562.
- 16 (a) Q. Sun, Y.-Q. Wang, A.-L. Cheng, K. Wang, E.-Q. Gao, *Cryst. Growth Des.* 2012, **12**, 2234; (b) X.-L. Sun, Z.-J. Wang, S.-Q. Zang, W.-C. Song, C.-X. Du, *Cryst. Growth Des.* 2012, **12**, 4431; (c) Y.-N. Zhang, P. Liu, Y.-Y. Wang, L.-Y. Wu, L.-Y. Pang, Q.-Z. Shi, *Cryst. Growth Des.* 2011, **11**, 1531; (d) M.-L. Han, J.-G. Wang, L.-F. Ma, H. Guo, L.-Y. Wang, *CrystEngComm* 2012, **14**, 2691.
- 17 (a) K. M. Blake, C. M. Gandolfo, J. W. Uebler, R. L. LaDuca, *Cryst. Growth Des.* 2012, **12**, 5125; (b) C. Li, D.-S. Li, J. Zhao, Y.-Q. Mou, K. Zou, S.-Z. Xiao, M. Du, *CrystEngComm* 2011, **13**, 6601.

## Graphical Abstract

Two unique entangling Cd (II) coordination polymers have been modulated by flexible/semi-rigid mixed-ligands systems. Notably, **1** shows the first topological motif of mutual-embedded bilayers originating from two reverse 2D  $4^4$ -*sql* layers with 1D single side arms, and thus affording a rare 3D polythreaded poly-pseudo-rotaxane structure and a new 3D (3,3,3,3,3,5,5,5)-connected self-penetrated H-bonding net. Whereas **2** displays a rare 2D→2D homochiral interpenetrated layers propagating from  $4^4$ -*sql* chiral layer.

